ISSN 2616-5667 Vol.3, Issue 3: 19-27, DOI: 10.25236/AJETS.2020.030304

Optical Fiber Humidity Sensor Based on Graphene Oxide

Huo Shihang[1, a], Tao Yuan[2, b]

[1]*harbin University of Science and Technology, Harbin 150080, China*
[2]*Harbin University of Science and Technology, Harbin 150080, China*
[a] *c12568012@163.com,* [b] *1241450339@qq.com*

ABSTRACT. *Based on the hydrophilic and humidity-sensitive characteristics of graphene oxide, the project combines it with optical fiber to study the real-time on-line humidity monitoring technology of optical fiber-graphene oxide. The sensor uses side polished optical fiber (SPF) as a substrate and graphene obtained by an improved oxidation-reduction method as a sensitive material. rGO is deposited in the polishing zone of SPF by natural evaporation deposition method, so that rGO interacts with optical field of optical fiber. Theoretical analysis of the sensing mechanism can explain the experimental results and show that the graphene-based optical fiber sensor can also be widely applied to the detection of other kinds of chemical gases. The experimental results show that the sensor has a linear response with sensitivity as high as 0.165 dB/%RH in the measurement range of 35% ~ 65% RH, so it has the advantages of high sensitivity and simple structure.*

KEYWORDS: *Graphene oxide, Optical fiber optics, Optical fiber humidity sensor, Side polished fiber*

1. Introduction

Graphene is a carbon film with only a few layers of atoms. Since it was separated from graphite crystals by mechanical peeling in 2004 [1], it has quickly become a research hotspot. As a two-dimensional semiconductor crystal, graphene has many unique electrical and optical properties, such as the bipolar field effect [2], the quantum Hall effect at room temperature [3], and extremely high charge mobility [4] , Support new electromagnetic propagation modes and so on [5]. The area in the optical fiber where part of the cladding is polished off is called polishing area. In the polishing zone, the optical field originally confined to the core leaks outside the fiber in the form of evanescent field, resulting in the interaction between the external environment and the optical field. Grapheneoxide (rGO) is graphene with oxygen-containing functional groups, so it has strong hydrophilicity [6]. The structure of rGO is a randomly stacked thin film. The adsorbed water molecules enter the gap between rGO layers. The intensity sensitivity of the optical fiber surface plasmon resonance humidity probe coated with polyvinyl alcohol (PVA) containing oxygen functional groups between rGO layers reaches 1.59%/%RH [7]; SMF melt taper is coated with PVA film and has a temperature compensated optical fiber humidity sensor to form a hydrogen bond network [8]. Reduced graphene oxide (rGO) is a kind of graphene prepared by chemical methods. Due to its lower production cost and higher output, it is widely used to make sensors [9].

When graphene is combined with an optical waveguide, the optical frequency conductivity of graphene will affect the effective refractive index of the optical waveguide, thus affecting the transmission light field in the optical waveguide. Humidity sensitive materials determine the sensitivity and response range of optical fiber humidity sensors, and are especially critical to their performance. Graphene oxide inherits the two-dimensional layered structure of graphene and has a large specific surface area [10]. Because graphene has extremely high thermal conductivity and highly sensitive temperature response characteristics [11], graphene-based optical fiber temperature sensors have the advantages of fast response speed, high sensitivity and the like. The hydroxyl group and epoxy group on the surface of the rGO layer form an oxygen bond network through hydrogen bonding, which leads to the increase of the rGO layer spacing and the expansion of the rGO film volume. In this paper, it is found that the side polished fiber (SPF) has piecewise monotonic response to humidity changes, and its characteristics in sensitivity, response speed and recoverability are studied. The sensing mechanism of the side polished fiber (SPF) is analyzed theoretically, and the application prospect of this new sensor in other chemical gas sensing is discussed.

2. Structure and Principle of Sensor

An on-line fiber M-Z interferometer is constructed by splicing the two ends of side polished fiber (SPF) with SMF through peanut-shaped fiber structure and dislocation fusion respectively. The obtained pure rGO powder was mixed in ultra-pure water and treated with ultrasound for 3 hours, and the large rGO particles were decomposed and peeled off into nanosheets. The pH value of rGO suspension was adjusted to 11 by using ammonium hydroxide with a mass fraction of 5%. Reducing graphite oxide to obtain rGO. Dispersing rGO in ultra-pure water, and treating with ultrasonic wave for 3h to make large pieces of rGO into flaky nanoparticles; Then taking out the supernatant, removing large pieces of rGO by a centrifugal separation method, and leaving small pieces of rGO solution; The reflecting surface is a thin film or other optical fiber at a certain distance from the end surface of the optical fiber. Based on the principle of double-beam interference, when light is transmitted to the graphene oxide film through a single-mode optical fiber, part of the light is fresnel reflected at the end face of the optical fiber, and the other part of the light reaches the contact surface of the graphene film and air and is fresnel reflected as well. Then, the discharge time was modified to 1500 ms, and the enlarged regions of lumbar vertebrae on both sides were realigned axially and welded. The size

ISSN 2616-5667 Vol.3, Issue 3: 19-27, DOI: 10.25236/AJETS.2020.030304

of this rGO monolithic piece was about 2mm×4mm, and the electrical conductivity was about 1.43×102S/m. rGO is mixed in high purity alcohol to form a suspension (10grGO per 100mL of alcohol).

Fig.1 Sensor Diagram

The graphene oxide humidity sensitive film is uniformly plated on the SPF surface by deposition. The depth of the polishing zone is 60 mm (i.e. the polishing surface has entered the core of the fiber about 1.5 mm) and the length of the polishing zone is about 1 cm. Place the optical fiber polishing section on the glass slide with the polishing surface upward, and form a groove with a size of about 2.5 cm×1 cm×0.1 cm around the optical fiber polishing section with ultraviolet glue, as shown in fig. 1. The polishing depth was measured with a filament measuring instrument (model XS-01-05-001) with an accuracy of 0.1μ m. Cut the purchased samples into squares with a size of 3mmx3mm, and place them on the surface of FeCl 3 solution as far as possible when placing them in corrosive solution so as to accelerate corrosion. After three hours of corrosion, NI-based exfoliation and graphene exfoliation from the sample can be observed. The random nature of deposition makes the thickness of the rGO film range from 200 nm to 1000 nm. During the coating process, part of the light energy of the laser in the optical fiber structure is converted into heat energy due to loss, which causes the local temperature to rise, and the solubility of the graphene oxide sheet layer is reduced and then precipitated and deposited on the SPF surface [12].

When the incident light passes through the peanut-shaped structure, part of the light propagating in the core is coupled into the cladding to excite the cladding mode propagating in the cladding. unpolished single mode fiber (SMF), SPF in bare air, SPF covered with graphene. The temperature in the constant temperature and humidity box is set at 25℃ and remains unchanged, while the relative humidity (RH, fRH) rGOes through a cycle, i.e. gradually increases from 40% to 95%, then gradually returns to 40%, with the adjustment range of 5% for each step. The remaining thickness of the cladding layer can not only ensure that the loss of polished optical fiber is small, but also ensure that the optical field has enough evanescent field to interact with graphene to ensure the sensitivity of the sensor. The refractive index change of graphene oxide film on its surface only affects the effective refractive index of cladding mode.

ISSN 2616-5667 Vol.3, Issue 3: 19-27, DOI: 10.25236/AJETS.2020.030304

In the process of SPF fiber core, the effective refractive indexes of the core mold and the cladding mold are changed, resulting in a reduction in the phase difference between the two, so the coating range is controlled on the surface of SPF. Further, the phase difference between the cladding mold and the core mold can be expressed as [13].

$$\Delta\Phi = \frac{2\pi\Delta n_{eff}^{m} L}{\lambda} \quad (1)$$

In formula (1), $\Delta n_{eff}^{m} L$ represents the effective refractive index difference between the core mold and the m-th order cladding mode, l is the length of SPF, λ is the wavelength of light, and the intensity of light output by m-z interference is as follows:

$$I = I_{\omega} + I_{d} + 2\sqrt{I_{\omega} I_{d}} \cos(\Delta\Phi) \quad (2)$$

In formula (2), and respectively represent the light intensity of core and cladding modes.

When the environmental humidity changes, the graphene oxide film adsorbs or releases water molecules. The water molecules act as electron acceptors to increase the surface charge density and Fermi level of graphene oxide materials, thus reducing its chemical potential. The humidity curve shows some fluctuations in each period of stable humidity retention, which is caused by small feedback adjustment of the constant temperature and humidity box during the humidity retention period. There are 1 ~ 2 μ m undulations in the polishing plane, which increases the scattering loss of the optical fiber. Based on the water absorption characteristics of graphene, when the humidity in the environment changes, the graphene material expands or contracts to change the sensor cavity length, thus causing the optical path change. Therefore, the interference curve will shift with the humidity change in the environment.

3. Experimental Results and Discussion

The humidity sensing experimental device consists of a highly stable laser light source (1550 nm), a 1×3 optical coupler, a constant temperature and humidity box with adjustable temperature and humidity, three optical power meters and a computer. The other humidity/thermometer used as a standard is also put into the constant temperature and humidity box to measure real-time humidity. The optical fiber humidity probe is fixed on the optical platform by a clamp and placed in a semi-sealed constant temperature and humidity box with an external dimension of 80 cm× 60 cm× 60 cm. The temperature and humidity calibrator is close to the optical fiber coating area. Each change is 10℃ and each temperature is maintained for at least 20 min. In order to ensure enough time for the three kinds of optical fiber samples to reach the temperature of the incubator. The interference spectrum signal carrying cavity length

ISSN 2616-5667 Vol.3, Issue 3: 19-27, DOI: 10.25236/AJETS.2020.030304

information reflected by the sensor is coupled to the spectrum analyzer again through the transmission fiber and the circulator, and the obtained interference spectrum is analyzed and calculated. As shown in Figure 4.

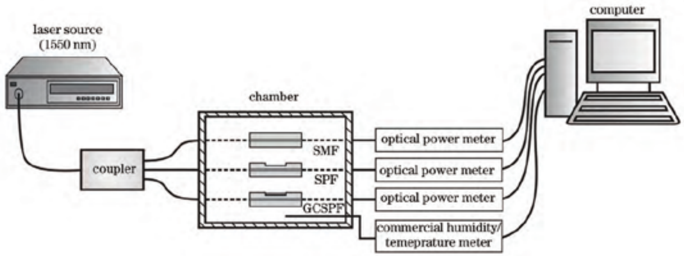

Fig.2 Experimental Setup Diagram

The three output ends of the optical coupler are respectively connected with three optical fiber samples: unpolished single mode fiber (SMF), SPF in exposed air, and SPF covered with graphene. The method can intuitively reflect the distribution of graphene oxide sheets on the surface of the optical fiber, and selecting a larger sheet diameter (larger than 500 nm) is beneficial to improving the moisture absorption capability of the graphene oxide film; On the other hand, the temperature increase intensifies the scattering effect of phonons on electrons and holes, resulting in an increase in the scattering rate of electrons and holes, resulting in a decrease in the dynamic conductivity of graphene. Each step includes a transition time (about 2min) and a time to stabilize at a set humidity (about 10min). Energy is mainly concentrated in the core mode and the cladding mode with the highest intensity, while the intensity of the higher-order cladding mode is relatively weak. It can be considered that the M-Z interference mainly occurs between the core mode and the cladding mode with the highest intensity, which is dominant. Therefore, the variation of the transmitted optical power of the standard optical fiber with time is caused by the stability factor of the laser itself, independent of the external temperature, and can be used to monitor the optical power of the light source.

We take the minimum sound pressure value detected by the sensor as the minimum value of the dynamic range of the detection system, and the sound pressure value when the total harmonic distortion is 3% as the maximum value of the dynamic range of the detection system to obtain the dynamic range of the demodulation method. The output light power is almost unchanged, which reflects that the humidity change has no influence on it and that the light source is stable. Fig. 3(a) is a time domain waveform diagram of the demodulated signal at a sound pressure frequency of 1 kHz and a sound pressure intensity of 280 mPa. fig. 3(b) is a frequency domain power spectrum diagram of the demodulated signal at a spectral resolution bandwidth of 2 Hz. the signal-to-noise ratio at the fundamental frequency of 1 kHz is 92.5 dB, and the calculated minimum detected sound pressure is 4.7 μPa/Hz1/2, with a corresponding sound pressure level of -12.6 dB (ref 20 μPa). In the environment of

ISSN 2616-5667 Vol.3, Issue 3: 19-27, DOI: 10.25236/AJETS.2020.030304

low humidity (20% ~ 35% RH), because the water molecules are not enough to penetrate graphene oxide film, the refractive index of the optical fiber surface changes little, so the interference intensity changes little. The change of the environment RH causes the interference spectrum to drift to a large extent, and the wave trough wavelength of the interference spectrum has a positive linear correlation with RH, which accords with theoretical analysis. In order to see the change rule of interference spectrum with RH more intuitively, the drift rule of wave trough wavelength with humidity is further analyzed.

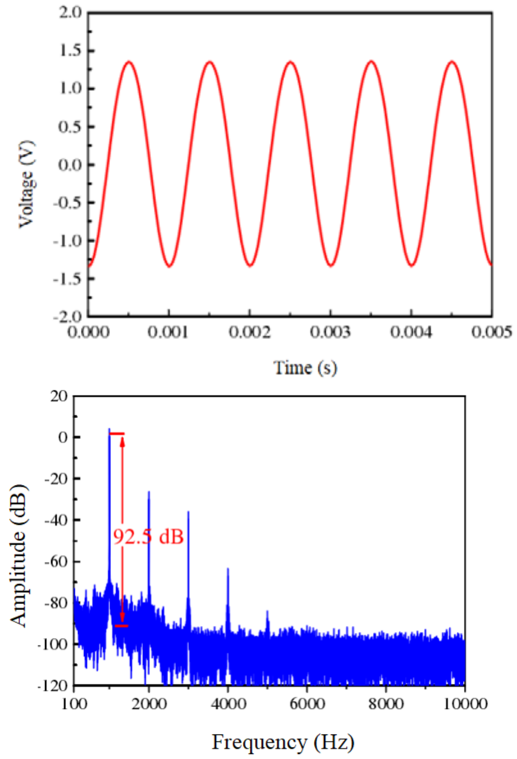

Fig.3 Demodulated Signal Time Domain Waveform Diagram; (B) Frequency Domain Pow Spectrum of Demodulated Signal

From fig. 4, the relationship between the relative output optical power and the relative humidity of SPF can be obtained. the decomposition temperature of graphene oxide (about 160℃) is higher than the temperature at which water is completely vaporized, so its refractive index is not sensitive to temperature changes at normal temperature. in the figure, small hollow squares and hollow circles respectively represent the temperature and relative transmitted optical power measured experimentally during the temperature rise and fall. In the humidity reduction stage,

ISSN 2616-5667 Vol.3, Issue 3: 19-27, DOI: 10.25236/AJETS.2020.030304

when the relative humidity is reduced from 95% to 70%, the relative output optical power drops steeply (about 6.93 dB); When the relative humidity decreases from 70% to 40%, the relative output optical power increases slowly (about 1.29 dB). Thereby affecting the splitting ratio and generating the intensity change of interference fringes; At the same time, SPF also underGOes thermal expansion and affects the phase difference between cladding mode and core mode. During the temperature change cycle, the standard error of transmitted light power measured experimentally is very small, and the maximum standard error is only 0.004 dB, which indicates that this temperature sensor is very stable. The red solid line and the black dashed line are the linear fitting curves of the transmitted light power with the change of temperature in the process of temperature rise and fall respectively.

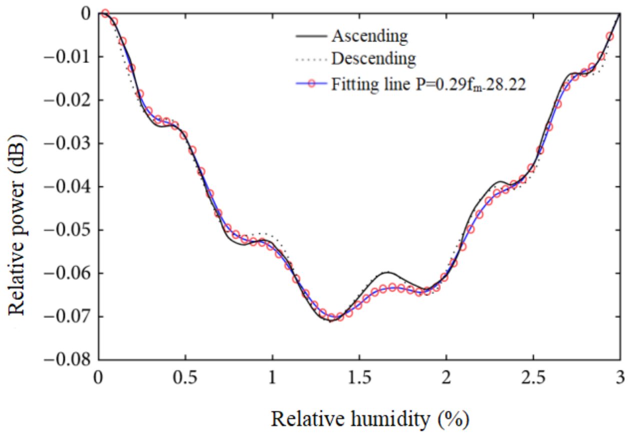

Fig.4 Figure Showing the Relationship between Spf Output Optical Power and Relative Humidity

The time domain waveform diagram of the interference signal including the measured signal output through the 3x3 fiber coupler is shown in fig. 5 below. even after a long time (thousands of seconds), the SPF output optical power cannot return to the initial value. At the same time, it also shows that SPF's recoverability to humidity increase is better than that to humidity decrease. Linear fitting shows that the relative optical power transmitted through the sensor has a rGOod linear dependence on temperature. The phase demodulation method of 3×3 fiber coupler can demodulate the measured signal well. In order to verify that the change of the initial phase has no influence on the phase demodulation alrGOrithm of the 3×3 fiber coupler, the sensitivity of this temperature sensor is 0.134 dB/℃ from the fitting equation. The measured maximum standard error is 0.004 dB. According to the sensitivity, the temperature measurement accuracy of this sensor is 0.03℃. In order to reduce the temperature cross-sensitivity of the sensor, the sensor and fiber grating can

ISSN 2616-5667 Vol.3, Issue 3: 19-27, DOI: 10.25236/AJETS.2020.030304

be connected in series to realize temperature compensation so as to improve the stability of humidity measurement.

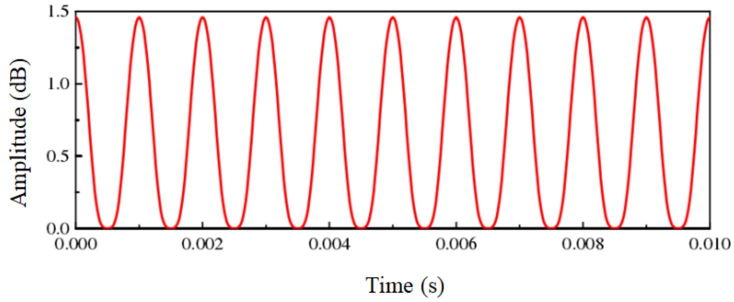

Fig.5 The Output Time Domain Waveform Diagram

Considering the piecewise monotonic response to humidity, SPF can be used for sensing in a certain local humidity range, for example, RH is 75%~95%. If the fluctuation signal with an amplitude of 0.5℃ is to be well reproduced, the temperature measurement accuracy of the sensor should be at least 1/10 of 0.5℃, i.e. 0.05℃. If the fluctuation signal with an amplitude of 0.5℃ is to be well reproduced, the temperature measurement accuracy of the sensor should be at least 1/10 of 0.5℃, i.e. 0.05℃, which is close to the value obtained by the above analysis. From this, it can be concluded that the sensitivity of the sensor to RH changes is 91.8pm%-1, and it has higher sensitivity to external humidity changes. According to whether the chemical gas is an electron “donor” type or an electron “acceptor” type, the output optical power response of SPF will be slightly different in low concentration detection. However, in the case of high concentration detection, the output optical power response of SPF will be similar to that described herein.

4. Conclusions

A new type of optical fiber humidity sensor is fabricated by depositing a layer of rGO film on the polishing surface of SPF, which has the characteristic of piecewise monotonic response to humidity changes. An on-line optical fiber M-Z interferometer is constructed by using peanut-shaped optical fiber structure and dislocation fusion technology. SPF is used in the middle and graphene oxide film sensitive to humidity is uniformly plated on the surface. The maximum transmitted light power can reach 11.3 dB at the experimental temperature ranging from-7.8℃ to 78℃, and has rGOod repeatability, which can be used as a temperature sensor. It not only helps to overcome the shortcoming of slow response and recovery speed of graphene electrochemical sensors and the limitation of limited detection at low concentration, but also has the advantages of simple manufacture, low cost, remote sensing, electromagnetic interference resistance, easy reuse, etc. But also has the advantages of simple manufacture, low cost, long-distance sensing, electromagnetic interference

ISSN 2616-5667 Vol.3, Issue 3: 19-27, DOI: 10.25236/AJETS.2020.030304

resistance, easy reuse and the like, and has important significance in the fields of food, environment, medical treatment and the like.

References

[1] Liu Zhigang, Yu Shihua, Geng Yijia, et al (2016). Design and application of SERS fiber optic sensor with solid-phase microextraction function. Spectroscopy and Spectral Analysis, S1, PP. 315-316.

[2] Xing Xiaobo, Chen Yilin, Liu Shaojing, et al (2016). Research and application of photothermal capture based on micro / nano fiber. Journal of South China Normal University (Natural Science Edition), vol 48, no. 5, pp. 15-18.

[3] Wu Xiaoxiao, Liao Wenying, Cao Xuewei, et al (2016). High birefringence characteristics of graphene-clad photonic crystal fibers. Acta Photonica Sinica, vol. 45, no. 1, pp. 106002-0106002.

[4] Yang Guang, Lou Jiachang, Han Daming, et al (2015). Passive Q-mode mode-locked erbium-doped fiber laser based on tapered fiber graphene saturable absorber . China Laser, vol. 42, s1, pp. 79 -83.

[5] Bi Weihong, Wang Xiaoyu, Fu Guangwei, et al (2015). Research progress of graphene-based optical modulators. Journal of Yanshan University, vol. 3, pp. 189-198.

[6] Hu Ping, Liu Fangfang, Huang Yan, et al (2019). Research developments in short-pulse fiber lasers based on two-dimensional materials. Laser and Infrared, vol. 049, no. 7, pp. 794-800.

[7] Xie Xiaohui, Huang Fazhong, Yue Weiwei (2019). Design of Fiber Optic Graphene FET Sensor and Its Application in pH Detection. Journal of Shandong Normal University (Natural Science Edition), vol. 034, no. 2, pp. 174-179.

[8] Chai Jing, Liu Qi, Zhang Bo, et al (2018). Research on temperature and humidity coupling of physical model materials based on fiber optic humidity sensor. Journal of Xi'an University of Science and Technology, vol. 2, pp. 210-216.

[9] Miao Jie (2017). Research on Calibration Method of HMP155A Temperature and Humidity Sensor [J]. Science and Information Technology, vol. 3, no. 031, pp 82-84.

[10] Pan Jinsheng, Li Renhui, Zhai Shuang, et al (2017). Research on monitoring system of urban box transformer based on fiber grating OPPC [J]. Electronic Quality, vol. 5, pp. 99-105.

[11] Ge Yuping (2017). Preliminary Study on Technical Problems of Fiber Optic Humidity Spherical Cavity Sensor Acquisition and Calibration Combination Device. Journal of Light Scattering, vol. 29, no. 2, pp.172-176.

[12] Li Delu, Chen Hongzhen, Zhang Gang, et al (2017). Design of traffic light timing control system based on temperature and humidity sensor. Automation and Instrumentation, vol. 7, pp. 82-83.

[13] Xiang Meiqiong, Liu Yanyang, Qing Xianguo, et al (2019). Application research of optical fiber sensing technology in nuclear power plant. Automation Instrumentation, vol. 6, pp. 132-136.